Fiber Deflection Probe Uncertainty Analysis for Micro Holes

Bala Muralikrishnan and Jack Stone

Abstract: We have recently reported on a new probe, the Fiber Deflection Probe (FDP), for diameter and form measurement of large aspect ratio micro-holes (100 µm nominal diameter, 5 mm deep). In this paper, we briefly review the measurement principle of the FDP. Then, we discuss different error sources and present an uncertainty budget for diameter measurements. Some error sources are specific to our fiber probe such as imaging uncertainty, uncertainty in determining calibration factor, and misalignment of the two optical-axes. There are other sources of error that are common to traditional coordinate metrology such as master ball diameter error, tilt in hole's axis, temperature effects etc. Our analysis indicates an expanded uncertainty of only 0.07 µm on diameter.

1. Fiber Deflection Probing

The stylus and probing system of a traditional Coordinate Measuring Machine (CMM) is limited at the low end of its measurement range because of large stylus diameter and high contact forces. In order to measure micro features and small holes of the order of 100 µm diameter, novel low force probing technologies are required. There are several such systems reported in the literature, which are summarized in a recent review by Weckenmann *et al*. [1]

Bala Muralikrishnan
Department of Mechanical Engineering & Engineering Science
University of North Carolina at Charlotte
9201 University City Blvd, Charlotte NC 28223 USA
(Guest Researcher, National Institute of Standards and Technology)
Email: bmuralik@uncc.edu

Jack Stone
Precision Engineering Division
National Institute of Standards and Technology
100 Bureau Drive, MS 8211, Gaithersburg, MD 20899 USA

At the National Institute of Standards and Technology (NIST), we have developed a new probing system for measuring holes of diameter 100 µm. We refer to this technique as Fiber Deflection Probing (FDP) and it is based on imaging a thin fiber stem using simple optics. The advantages of this technique are the large aspect ratio achievable (5 mm depth in 100 µm hole), an inexpensive probe that can be easily replaced, large over-travel protection of approximately 1 mm before probe damage, extremely low contact force ($\approx$ 1 µN) to avoid part damage, and extremely small uncertainties (0.07 µm, k = 2 on diameter).

The measurement principle is shown in Fig. 1(a). A thin fiber (50 µm diameter, 20 mm long), with a microsphere (80 µm diameter) bonded on the end, serves as the probe. The deflections of the stem upon contacting a surface are detected by optically imaging the stem, a few millimeters below the ball. The

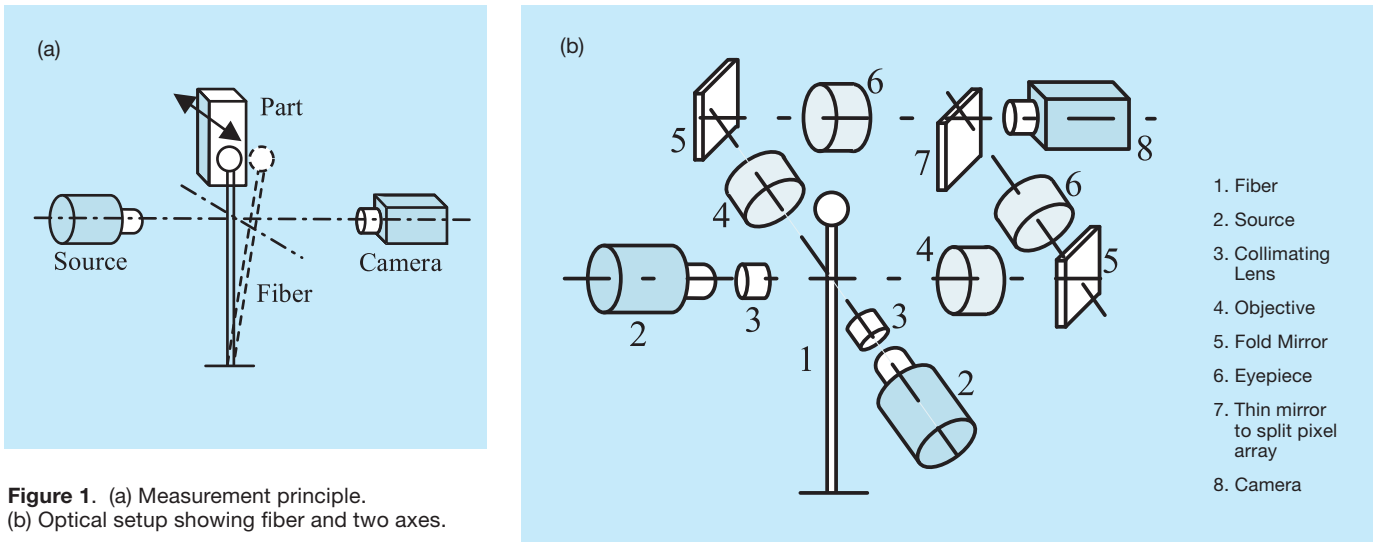

Figure 1. (a) Measurement principle. (b) Optical setup showing fiber and two axes.

optical setup used is shown in Fig. 1(b). The stem of this fiber is illuminated from two orthogonal directions to detect deflections in *X* and *Y*. The resulting shadows are imaged using objectives and a camera. Upon contact with a test surface, the fiber deflects and also bends. By determining the position of the fiber in the deflected state and also in the free state, and using a previously determined scale factor (in units of µm/pixel) that accounts for both the bending and deflection, we can correct the machine's final coordinates to determine surface coordinates. The probing system is currently a heavy prototype that is placed on the bed of the machine, with the probe pointing upwards. All measurements are carried out on the Moore M48 [2] measuring machine at NIST. The machine is used primarily as a fine three-axis positioning stage; its Movamatic probing system is removed from the ram to allow the placement of the test artifacts. A detailed description of the technique along with validation results and small hole measurement data can be found in [3]. Here, we discuss different error sources involved and provide an uncertainty budget for diameter measurements.

2. Error Sources Overview

We provide an overview of the different sources of error in measuring artifacts such as a small hole. In subsequent sections, we describe them in greater detail and tabulate an uncertainty budget.

Sources of error that are specific to our fiber probe:

1. As mentioned in the previous section, we determine any coordinate on a surface from knowledge of the fiber's free and deflected state and the machine coordinates at the deflected state. There is an uncertainty in determining both the machine's position at the deflected state and the fiber's position (imaging uncertainty). This contributes to an uncertainty in determining every coordinate in space and consequently impacts diameter.
2. In order to determine the magnitude of the fiber's deflection in units of length, we require a scale factor that converts the fiber's deflection in pixels to micrometers. Uncertainty in determining the scale factor will contribute to an uncertainty in part diameter, not directly but in combination with other factors as described in Sections 3.2 and 4.
3. The two optical axes of the fiber probe are not necessarily aligned with the machine's axes. This non-orthogonality/misalignment introduces an error in diameter. We typically compensate this term in software, but a small residual can remain.

Other general sources of error:

1. As with any traditional coordinate measurement process, we have to calibrate the probe ball diameter (and form) using a master ball of known diameter (and form). The uncertainty in master ball diameter is therefore another term in our budget.
2. Uncertainty in determining the equatorial plane of the master ball and tilt angle of the test hole contribute to an uncertainty in final diameter.
3. Temperature effects are not significant for dimensional measurement of small holes, but may impact master ball diameter measurement.

For purposes of this error budget, we consider a 3000 µm nominal diameter ruby sphere as the master ball and a 100 µm nominal diameter ceramic hole as the test artifact. All results are based on Least Squares (LS) algorithm with 16 points sampled along the surface. Nominal probe ball diameter is assumed to be 80 µm.

3. Uncertainty in Determining a Coordinate in Space – *u(coordinates)*

3.1 Errors in Determining Fiber Center by Shadow Imaging

While an uncertainty budget for diameter measurements is presented later on, we discuss the uncertainty in determining the fiber center due to imaging here. This term, along with the machine's positioning repeatability, is used later to determine the uncertainty in obtaining any coordinate in space. Figure 2(a) shows two thin white bands of light that represent a portion of the fiber stem viewed from two orthogonal directions. (The glass fiber behaves as a cylindrical lens and focuses light on the image plane to produce the bands; we monitor the position of these bands instead of the outer boundaries of the shadow. One

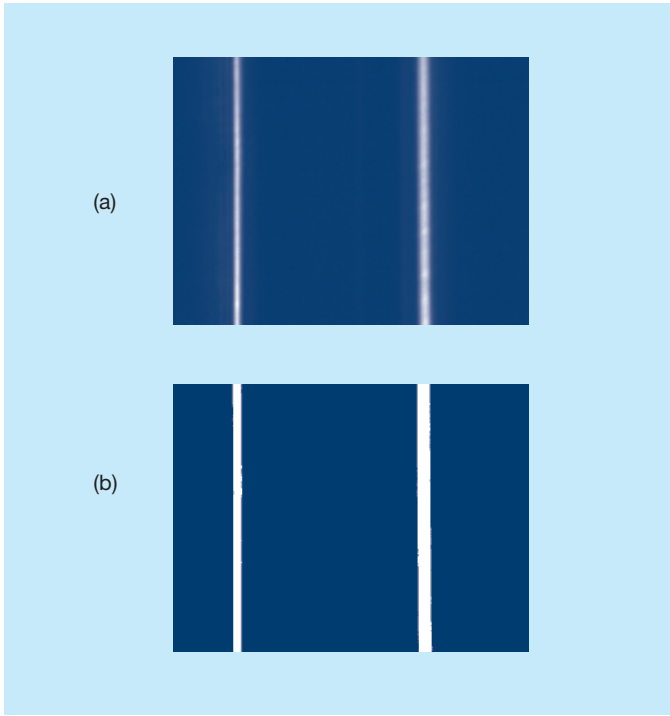

Figure 2. (a) Image as recorded by the camera. (b) Binary image after processing.

band corresponds to motion along *X*, another to motion along *Y*). These bands after image processing are shown in Fig. 2(b). We determine a center position for the stem (in pixel coordinates) in each direction by least squares fitting (using data from an edge finding routine applied to each row) and averaging (left and right edge for each band).

We use a 640 by 480 pixel array Charge Coupled Device (CCD) camera, where the width of each pixel is 8500 nm. With an optical magnification of 35, the pixel resolution is 8500/35 = 243 nm. Therefore, the center can lie within – 122 nm and +122 nm with equal probability. Assuming a rectangular distribution, the standard uncertainty is $122 / \sqrt{3} = 70$ nm. This is the uncertainty in determining the center using just one row of pixels. We average over 400 rows (out of the total possible 480 rows, a few are discarded because of outliers) to reduce this uncertainty. In the absence of noise, a slight tilting of the fiber relative to the field of view is needed to average over the quantization error of discrete pixels; this is a very standard imaging technique that has close analogs in other fields such as electronics [4]. The mathematical details differ slightly from one implementation of the technique to the next depending on the averaging algorithm employed (for us, the least squares fit). The reduction in uncertainty due to averaging is a complex function of the angle of the fiber relative to the pixel array. If the fiber is misaligned relative to the pixel array so that it crosses more than three pixels in the horizontal direction, then the error due to pixel resolution is reduced below ±0.04 pixels (±10 nm). Assuming a rectangular distribution of errors, this ±10 nm range of possible errors corresponds to a standard uncertainty of 6 nm. For some angles the uncertainty might be considerably smaller, but as long as the angle is large enough that at least three horizontal pixels are crossed, the uncertainty will not exceed this value. Also, as a consequence of the fact that we measure both the left and right edge of the band, the uncertainty will be reduced to a value on the order of $(6 / \sqrt{2})$ nm = 4 nm. Thus we might hope to see roughly a 4 nm (which is equivalent to about 0.015 pixels, at a nominal scale factor of 300 nm/pixel) uncertainty in detecting the position of the probe in space under ideal conditions. We have carried out measurements that indicate that this small uncertainty for the imaging system is probably attainable, but under realistic conditions our uncertainties are much larger, with the imaging uncertainty contributing negligibly to the overall uncertainty budget. Although the 4 nm uncertainty might be improved further by sophisticated subpixel interpolation, there is no practical advantage to doing so.

3.2 Uncertainty in Determining a Coordinate in Space

The coordinate of any point on the surface is determined from knowledge of the fiber center in both the free state and in the deflected state. We know the machine's coordinates at the deflected state and the magnitude of the fiber's deflection. From these, we can infer the coordinates of the center of the probe tip when it is in contact with the surface. Thus, the final coordinate (*X, Y*) on the surface after correcting for the fiber's deflection is given by:

$$X = (P_x - P_{xo})*SF_x + X_o\,, \qquad (1)$$

$$Y = (P_y - P_{yo})*SF_y + Y_o\,, \qquad (2)$$

where (X_o, Y_o) are the CMM readings in micrometers at the deflected state of the fiber, (P_x, P_y) are the fiber centers in pixels at the deflected position, (P_{xo}, P_{yo}) are the fiber centers in pixels at the free undeflected state and SF_x and SF_y are the scale (or calibration) factors in µm/pixel along *X* and *Y*. The uncertainty in any coordinate (*X,Y*), given by $(u(X), u(Y))$, is therefore a function of uncertainties in each of the quantities on the right hand side of Eqs. (1) and (2) and is given by:

$$u^2(X) = c_{Px}^2 u^2(P_x) + c_{Pxo}^2 u^2(P_{xo}) + c_{SFx}^2 u^2(SF_x) + c_{Xo}^2 u^2(X_o)\,, \qquad (3)$$

$$u^2(Y) = c_{Py}^2 u^2(P_y) + c_{Pyo}^2 u^2(P_{yo}) + c_{SFy}^2 u^2(SF_y) + c_{Yo}^2 u^2(Y_o)\,, \qquad (4)$$

where the coefficients are the partial derivatives as described in the US Guide to the Expression of Uncertainty in Measurement. [5]

Before we proceed with the evaluation of the different uncertainties in the right hand side of Eqs. (3) and (4), we make the following observations/assumptions:

- First, we assume that the uncertainties are not directionally dependent. Therefore, $u(P_x) = u(P_y)$, $u(P_{xo}) = u(P_{yo})$ and $u(X_o) = u(Y_o)$. This simplifies our discussion to only terms on the right hand side of Eq. 3.
- Second, we observe that the uncertainties in scale factors, $u(SF_x)$ and $u(SF_y)$, have only a very small effect on typical measurements, where the measurements are performed at nearly the same deflection as used when the probe is calibrated. If the measured scale factor is smaller than the true

value, the master ball diameter appears smaller, resulting in a smaller value for the fiber probe ball diameter. Because we use the same scale factor for test artifact (small hole) measurement, the smaller scale factor, combined with a smaller probe ball diameter produces the correct hole diameter, in essence canceling out the effect of $u(SF_x)$ and $u(SF_y)$. Some error will remain because the probe deflection is not exactly the same for calibration and for test artifact measurement, but typically this is a small error. We discuss this source in Section 4.

- Third, determining the free state of the fiber is not critical because this term only serves to translate the center coordinates and does not influence diameter or form. Therefore, we can ignore the free state in all computations and simply report a coordinate as $X = P_x * SF_x + X_o$.

From this, the uncertainty in determining a coordinate can be simplified as:

$$u^2(X) = u^2(Y) = c_{Px}^2 u^2(P_x) + c_{Xo}^2 u^2(X_o) \ . \qquad (5)$$

Using $c_{Px} = \frac{\partial X}{\partial P_x}$ = 300 nm/pixel (nominal scale factor value), $c_{Xo} = \frac{\partial X}{\partial X_o}$ = 1, $u(P_x)$ = 0.015 pixels (from previous section) and $u(P_o)$ = 35 nm, the combined standard uncertainty in determining the X (and Y) coordinate of any point in space using the fiber probing technique is 35 nm. The uncertainty is dominated by $u(X_o)$, and the value given here for $u(X_o)$ was determined experimentally as the standard deviation of repeated measurements of a point on a surface. This lack of repeatability is large relative to other sources of uncertainty. The source of repeatability errors is still under investigation, but it is likely that they arise primarily from CMM positioning errors.

Note that we do not include probe non-orthogonality in Eq. (1) and (2) because we compensate for this error in software (see Section 9). We also do not treat non-orthogonality in CMM axes separately. The Moore M48 is well characterized and error mapped. Therefore, we do not separately treat its errors. Instead we lump motion related errors into one term: its single point repeatability of 35 nm. For a more detailed discussion of error sources and uncertainty budgets for the NIST Moore M48 CMM, we refer to [6].

3.3 Contribution of Uncertainty in Coordinates to Uncertainty in Diameter

The contribution of this term to diameter uncertainty is determined using Monte Carlo Simulation (MCS). [7] With 35 nm standard deviation Gaussian noise, and using 16 sampling points with a LS fitting routine, we determine the standard uncertainty in diameter to be 18 nm. This term is the largest contributor to the overall uncertainty budget, and affects every coordinate measured using the fiber probe. Therefore this term affects both the calibration and test artifact measurement.

4. Uncertainty in Scale Factor Combined with Unequal Fiber Deflection – *u(SF)*

As mentioned in Section 3.2, the uncertainty in the scale factor will not directly impact the final diameter if we use the same scale factor value for both the calibration and test artifact measurement. This is true under the circumstance that the fiber deflects by the same nominal amount at all angular positions (sampling locations) of both the master ball and test artifact. In reality, the fiber will not deflect by identical amounts at all angular positions of any artifact because of centering and part form error. Assuming a 2 µm centering error in the test artifact (the master ball is assumed to be well centered), a nominal scale factor of 300 nm/pixel, 0.5 nm/pixel standard uncertainty in the scale factor, and 15 µm nominal deflection, the uncertainty in diameter is 1 nm. Also, the fiber will not necessarily deflect by the same nominal amount for both the calibration and test artifact measurement. Assuming typical nominal deflections are held to within a 2 µm range between the calibration and test artifact measurement, the uncertainty in diameter is 7 nm.

5. Master Ball Diameter Uncertainty – *u(master)*

For purposes of calibrating the diameter (and form) of the probe ball, we use a 3 mm nominal diameter ruby sphere mounted on a stem (a CMM stylus), as the master ball. The diameter of this master ball is determined to be 3000.79 µm with a standard uncertainty of 5 nm using interferometry at NIST. The master ball diameter uncertainty was determined by measuring two point diameters at different locations and therefore samples some form error also.

6. Uncertainty in Determining Equatorial Plane of Master Ball – *u(height)*

Determining the equatorial plane of a sphere is important during calibration to obtain an accurate diameter of the probe ball. The equatorial plane is found iteratively as follows. We first determine the approximate center of the circle at some arbitrary plane near the equatorial plane. Using this center, we determine the location of the pole point along Z, and then evaluate the new location of the equatorial plane from knowledge of the ball's diameter. We repeat this process several times to refine the location of the equatorial plane. The error in determining the Z location of the equator is ±1.5 µm from this method. The standard uncertainty in determining calibration artifact diameter is therefore 1 nm.

7. Temperature Effects – *u(temperature)*

Temperature effects are typically not significant for dimensional measurement of small objects. If temperature can be controlled to within ±0.05 °C, the change in diameter is 0.8 nm for the master ball. The radial expansion of the probe tip and the test hole are negligible. Therefore, assuming a rectangular distribution, the standard uncertainty in determining master ball diameter because of non-standard temperature is 0.5 nm.

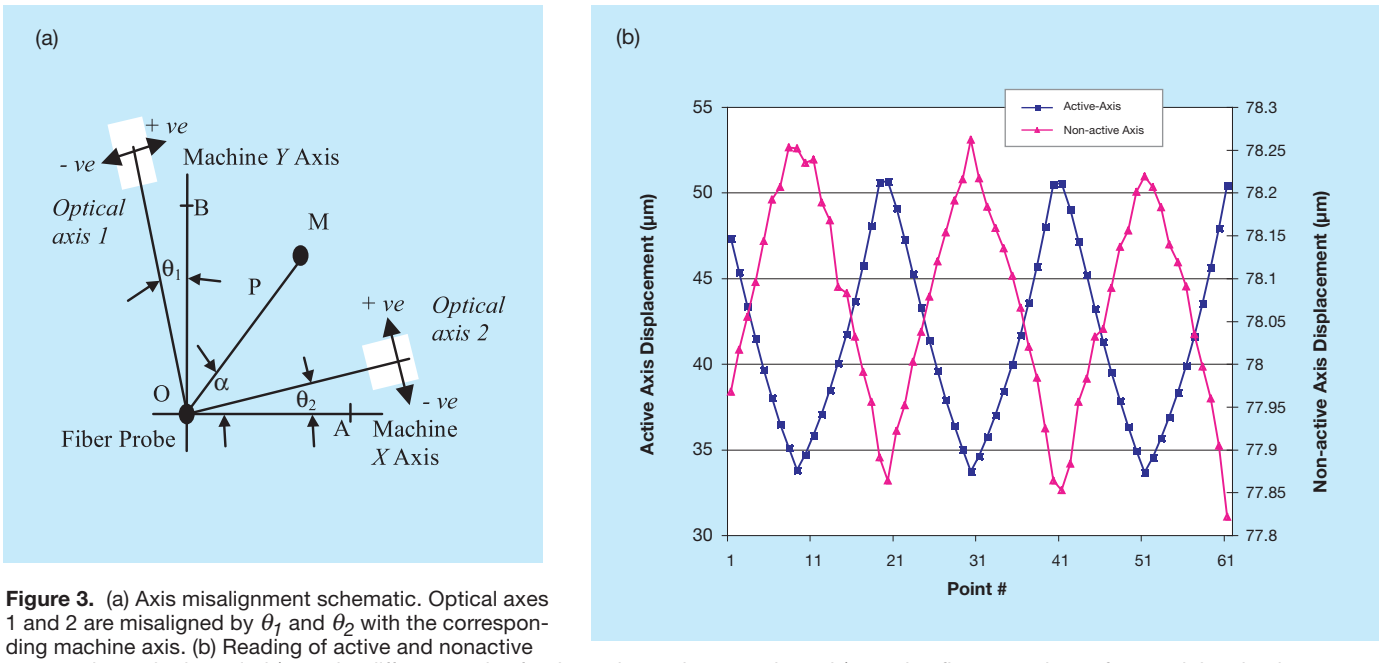

Figure 3. (a) Axis misalignment schematic. Optical axes 1 and 2 are misaligned by θ_1 and θ_2 with the corresponding machine axis. (b) Reading of active and nonactive axes as the probe is cycled (note the different scales for the active and non-active axis), moving first toward a surface and then back out from the surface. Positive θ is as shown in the figure. The sign conventions shown for each probe refer to pixel coordinates; that is, deflection of the fiber to the right of optical axis 1 is considered positive for that axis and deflection to the left for optical axis 2 is considered positive.

8. Uncertainty in Aligning Hole Axis with Machine's Z axis – *u(tilt)*

The tilt angle of a hole's axis affects final diameter values. Assuming tilt can be controlled to within ±0.5 °, the standard uncertainty in diameter is 1 nm.

9. Uncertainty in Aligning Optical Axis with Machine's X & Y axes – *u(AM)*

9.1 Introduction to Axis-misalignment

The two optical axes of the probe measurement system are not necessarily aligned with the machine's axes. This misalignment introduces an error in diameter (and form), which if uncompensated can be a significant portion of the total uncertainty budget. We discuss this error source and our approach to compensating it. A residual error will remain; it is itemized in the uncertainty budget. It is worthwhile to emphasize that these alignment errors, which are usually of only minor importance for measurements of typical engineering metrology artifacts, take on much greater significance when probe deflections are comparable in magnitude to machine motions, such as, for example, when measuring the inside diameter of a 100 µm hole with an 80 µm diameter probe.

Figure 3(a) shows a schematic of the measurement system. The fiber probe stem (top view) is shown at the origin, with the optical axis 1 misaligned with the machine's Y axis by θ_1, and the optical axis 2 misaligned with the machine's X axis by θ_2. When the machine deflects the probe along the X axis, optical axis 1 (which is aligned with the Y axis) senses the displacement and is therefore the X-axis sensor. The '+ve' and '–ve' signs show the sign convention in pixel coordinates as explained in the figure caption.

In a typical measurement process, the test part (either the master ball or the hole) is brought in contact with the fiber at a certain angle (α) and further translated by P along the same direction. If the two optical axes are perfectly aligned, axis 1 (that is, the X-axis sensor) senses a displacement of $P\cos\alpha$, while axis 2 senses a displacement of $P\sin\alpha$ (the sign conventions for the two optical axes are shown in Fig. 3). These displacements ($P\cos\alpha$, $P\sin\alpha$) are then corrected from the machine coordinates at that location to determine the coordinates on the surface. However, if the optical axes are aligned as shown in Fig. 3 (a), axis 1 senses a displacement of $P\cos(\alpha - \theta_1)$, while axis 2 senses a displacement of $P\sin(\alpha - \theta_2)$. The displacement corrections are therefore incorrect resulting in errors in part diameter and form.

Figure 3(b) shows experimental evidence of the presence of this error. As the part is brought in contact with the fiber along the machine's X axis and displaced back and forth in steps of 1.5 µm over a travel of 15 µm (active axis – optical axis 1 readings), optical axis 2 (non-active axis) records a motion of approximately 0.4 µm, indicating that optical axis 2 is not aligned with the machine's X axis.

9.2 Understanding its Impact

Axis misalignment can potentially be a large component of the overall error budget, if left uncompensated. In order to understand its impact, we consider two cases. If $\theta_1 = \theta_2$, the resulting coordinates after displacement correction are rotated to a new point, either inside or outside the true surface. Thus, the impact is only on diameter, not on form. (Form errors will occur, however, if there are variations in the magnitude of the probe displacement from point to point.) If $\theta_1 \neq \theta_2$, the resulting coordinates after displacement correction are not only rotated but also stretched and compressed along two orthogonal axis (causing an apparent ovality), resulting in errors in diameter and form.

Most of the misalignment induced errors cancel between the master ball and test hole measurement. There is however a residue, which is not insignificant, as shown here. Although probe errors that are strictly along the radial direction are independent of the diameter of the object being measured, errors along a direction tangent to the measurement direction have much greater influence on the calculated diameter when probe deflections become comparable to machine motions; in a diameter measurement, the tangential errors represent second-order cosine errors of negligible magnitude when measuring a circle of large radius but become much larger when measuring a very small circle. This effect is particularly important when the calibration artifact is macroscopic and the test artifact, a hole, is only slightly larger that the probe diameter. For a 5° misalignment angle in one axis, no misalignment in the other, the error in diameter when measuring a 3 mm ball (80 µm probe tip with 15 µm nominal deflection) is – 57 nm (diameter appears to be smaller for outer diameter features). For the same conditions, the error in diameter for a 100 µm hole is 121 nm (diameter appears to be larger for inner diameter features). Thus, if the 3 mm ball measurement is used to calibrate the probe tip diameter prior to a measurement of the diameter of the 100 µm hole, the net diameter error is 64 nm. Because the axes are not orthogonal, there is also a residual out-of-roundness error of approximately 86 nm. For a 0.5° misalignment in one axis, these numbers are much smaller. The residual errors in diameter and out-of-roundness are only 1 nm. Thus, if we can estimate axis misalignment angles to within 0.5°, our compensation will significantly reduce the contribution of this term to the overall budget.

Typically observed misalignment angles are between – 5° and + 5° in both axes (note that while these angles may seem large, these angles represent a combination of physical and optical misalignment). It is therefore necessary to compensate diameter and form for axis misalignment. We discuss next a procedure to evaluate the magnitude of this misalignment. Then, we discuss our approach to correcting for it.

9.3 Estimating Axis Misalignment Angles

Our procedure for estimating axis misalignment angles involves monitoring both optical axes while deflecting the fiber along two of the machine's principal directions. As mentioned earlier, if the optical axes are well aligned with the machine's axes, and the fiber is deflected along the machine's X axis, optical axis 1 senses all of the deflection while optical axis 2 senses no deflection at all. The same is true for deflections along the machine's Y axis, where optical axis 1 senses no deflection and optical axis 2 senses the complete deflection.

If however, the optical axes are aligned as shown in Fig. 3, then we follow the procedure outlined here to estimate θ_1 and θ_2. First, we let the test part contact (at point O, the origin) and deflect the probe (to point A) as the part moves along the machine's positive X direction. Let the deflection of the probe, OA, be P. Let the magnitude of the observed probe deflections by optical axis 1 and optical axis 2 be X_A and Y_A pixels. Also, let the scale factors in X and Y be S_x and S_y, expressed in units of µm/pixel if the deflection P is measured in micrometers. Then,

$$\begin{aligned} P\cos(\theta_1) &= X_A * S_x \\ P\sin(\theta_2) &= -Y_A * S_y \end{aligned} \tag{6}$$

We then contact the probe and displace it to point B along the positive Y direction, again by P. Let the magnitude of the observed deflection seen by optical axis 1 and optical axis 2 be X_B pixels and Y_B pixels. Then,

$$\begin{aligned} P\sin(\theta_1) &= X_B * S_x \\ P\cos(\theta_2) &= Y_B * S_y \end{aligned} \tag{7}$$

From Equations 6 and 7, we get:

$$\begin{aligned} \theta_1 &= \tan^{-1}(X_B / X_A) \\ \theta_2 &= \tan^{-1}(-Y_A / Y_B) \end{aligned} \tag{8}$$

S_x and S_y can also be obtained from these equations. Similar equations can be written for deflections in the opposite directions yielding another set of values for θ_1, θ_2. The results can then be averaged to obtain axis misalignment angles.

9.4 Compensating Axis Misalignment Error

After the angles are determined, we can estimate the magnitude of the correction as described here. Let the fiber be deflected by some distance at an arbitrary angle α. Let a and b be the observed readings (in pixels) of optical axis 1 and optical axis 2 respectively. Let u and v be the true deflections along the X and Y directions. Then u and v can be determined from the following system of equations:

$$\begin{aligned} u\cos(\theta_1) + v\sin(\theta_1) &= a \\ -u\sin(\theta_2) + v\cos(\theta_2) &= b \end{aligned} \tag{9}$$

Thus, from the observed deflection (a, b) at every angle α, we can determine the true deflection (u, v) and compensate for axis misalignment.

10. Other Miscellaneous Errors

Hertzian deformations of the probe tip and workpiece are negligible because measurement forces are only 0.16 µN when the probe is deflected by 20 µm. We have therefore not discussed this error source. A complete accounting of errors would also include a component due to incomplete sampling of the part form errors; for purposes of our discussion here we ignore this potential complication.

The emphasis in this paper has been on the fiber probe, and therefore we have not explicitly discussed CMM scale and positioning errors. For our M48 CMM, these errors (interferometric scale related and other machine errors) are primarily manifested as part of the 35 nm repeatability discussed previously. Previous studies of the M48 show that other positioning errors that would affect these small-scale diameter measurements (errors such as hysteresis or, more likely on the M48, errors of short spatial period associated with the roller bearings) might contribute as much as 20 nm uncertainty to a two-point diameter measurement at a particular spot on the table. This uncertainty should be reduced to 14 nm for a four-point diameter measurement that samples independent errors associated with measurements along the x and y axes. For two-artifact

measurement (master ball and test hole), this translates to an effective uncertainty of about 20 nm in diameter.

Finally, there are errors associated with dust settling on either the test part or the master ball. Dust is a persistent problem when using low-force probing outside of a clean room. Most often, a particle of dust will produce a large, obvious error, and can be corrected by cleaning, but if a very small piece of dust produced a radial error under 50 nm, this error might go undetected. However, it is unlikely that this would occur at more than 1 of the 16 measurement points, and therefore the resulting diameter error would be less than 3 nm.

Experimentally, we have determined the standard uncertainty in diameter to be of the order of 20 nm. This repeatability samples the different error sources we have outlined in previous sections. It is however possible that there are other sources we have not sampled, such as those described in this section and any other unknown sources. To account for these, we itemize a 20 nm uncertainty in diameter in our budget.

11. Summary: Overall Uncertainty Budget

Finally, we tabulate in Table 1 the contributions of the different sources towards the uncertainty in diameter for a 100 µm hole. From Table 1, the combined standard uncertainty in diameter is 34 nm. Thus, the expanded uncertainty is 0.07 µm (k = 2) on diameter.

Note that the uncertainty in diameter will be smaller than the uncertainty in determining a position (35 nm) because of the averaging involved. We sample 16 points along the circumference of a circle. The uncertainty in each coordinate is (±35 nm, ±35 nm). As explained in section 3.3, the uncertainty in diameter (based on 16 sampling points, LS best fit) is reduced to only 18 nm. Adding in other terms as shown in the uncertainty budget in Table 1, the final combined standard uncertainty in diameter is 34 nm.

Error Source	Description	Uncertainty (nm)
ucal(Coordinates)	Uncertainty in probe ball diameter due to uncertainty in determining coordinates (X, Y) of probing points. This is primarily because of imaging uncertainty and machine repeatability.	18
u(Coordinates)	Same as 1, but on test artifact.	18
u(SF)	Uncertainty in scale factor combined with centering error.	1
	Uncertainty in scale factor combined with unequal nominal deflections between master ball and test artifact measurement.	7
ucal (Height)	Error in determining the equatorial plane (Z height) on master ball.	1
ucal (Master)	Uncertainty in master ball diameter and form.	5
ucal (T)	Uncertainty in diameter due to nonstandard temperature. This affects calibration sphere diameter primarily because of larger nominal diameter. Test artifact diameter is much smaller and temperature effects are ignored.	1
u(Tilt)	Error in determining tilt angle on test artifact	1
u(AM)	Probe axis misalignment introduces an error in diameter, some of which cancels out when measuring the cal-ball and later the test artifact. Also, most of this error is software corrected. The residual error is tabulated here.	1
u(Other Sources)	Contribution from machine positioning and other sources.	20

Table 1. Error sources contributing to uncertainty in diameter. Expanded uncertainty is 0.07 µm (k = 2) on diameter. Note that the subscript 'cal' indicates calibration process.

12. Conclusions

We have discussed different error sources involved in measuring the diameter of 100 µm nominal diameter holes using a new fiber deflection probe for CMMs. The probing uncertainty, which is the imaging term, is of the order of 4 nm. Experimentally determined single point repeatability using the fiber probe, on a CMM is approximately 35 nm. A substantial portion of this rather large difference is attributable to the machine's positioning repeatability. However, we are still investigating the presence of any other systematic effects that might contribute to this loss in performance. Overall, our analysis indicates expanded uncertainty of only 0.07 µm (k = 2) on diameter. This value is amongst the smallest reported uncertainties in the literature for micro holes measured using a CMM. Our current focus is on expanding the technique to 3D and profile measurements and in understanding the error sources involved therein.

13. References

[1] A. Weckenmann, T. Estler, G. Peggs, and D. McMurtry, "Probing Systems in Dimensional Metrology," *Annals of the CIRP*, vol. 53, pp. 1-28, 2004.

[2] Commercial equipment and materials are identified in order to adequately specify certain procedures. In no case does such identification imply recommendation or endorsement by the National Institute of Standards and Technology, nor does it imply that the materials or equipment identified are necessarily the best available for the purpose.

[3] B. Muralikrishnan, J. Stone, S. Vemuri, C. Sahay, A. Potluri, and J. Stoup, "Fiber Deflection Probe for Small Hole Measurements," *Proc. of the ASPE Annual Meeting,* pp. 24-27, 2004.

[4] M.F. Wagdy, "Effects of Various Dither Forms on Quantization Errors of Ideal A/D Converters," *IEEE Trans. Instrum. Meas.,* vol. 38, pp. 850-855, 1989.

[5] "US Guide to the Expression of Uncertainty in Measurement," *ANSI/NCSL Z540-2-1997*.

[6] John Stoup and Ted Doiron, "Measurement of Large Silicon Spheres using the NIST M48 Coordinate Measuring Machine," *Proc. of the SPIE,* vol. 5190, pp. 277-288, 2003.

[7] M.G. Cox, M.P. Dainton and P.M. Harris, "Software Support for Metrology, Best Practice Guide No. 6: Uncertainty and Statistical Modeling," ISSN 1471–4124, NPL, UK, March 2001.